Phase Noise Metrology

Enrico Rubiola[1,2⋆] and Vincent Giordano[2⋆⋆]

[1] Politecnico di Torino, Dipartimento di Elettronica, and INFM UDR Politecnico c.so Duca degli Abruzzi no. 24, I-10129 Torino, Italy
[2] LPMO – UPR-3203 du CNRS associée à l'Université de Franche-Comté 32 Rue de l'Observatoire, F25044 Besançon, France

Abstract. As a result of a major technological trend towards high speed digital communications and circuits, phase noise turns out to be a relevant concern for scientists and engineers. This paper describes methods and instruments to measure the phase noise of oscillators, components and more complex devices in the radiofrequency and microwave bands, from approximately 100 kHz to 30–40 GHz, and even beyond. After a brief introduction, two sections deal with basic definitions and traditional methods, and one section presents a set of schemes that cover most actual needs. Then a new approach – known as the *interferometric method* – is discussed in detail, providing design strategies and examples; this method exhibits the highest sensitivity in real time, which can alse be exploited to dynamically correct the phase noise of amplifiers and oscillators. The last section deals with an improved version of the interferometric method, in which correlation is used to remove the instrument noise of two equal interferometers that simultaneously measure the same device. This scheme enables the measurement of low noise processes, even below the thermal floor, and therefore it represents the state of the art in the high sensitivity phase noise metrology.

1 Introduction

This paper deals with the measurement of the phase noise of radiofrequency and microwave signals. As one can expect, we are mainly interested in the measurement of *low noise* signals.

We first define a quasi-sinusoidal signal of the form

$$s(t) = \sqrt{2R_0P_c}\,[1+\alpha(t)]\cos[2\pi\nu_c t + \varphi(t)]\,. \tag{1}$$

were R_0 is the characteristic impedance and P_c is the carrier power. $\varphi(t)$ and $\alpha(t)$ are realizations of random processes that we call *phase noise* and (relative) *amplitude noise*, respectively. By definition $\alpha(t)$ and $\varphi(t)$ have zero mean, which results from an appropriate choice of P_c and of the time axis origin. Phase noise is our main concern, while amplitude noise can also be of interest in a smaller set of problems and applications. The phase noise is commonly described in terms of $S_\varphi(f)$, i.e. the power spectrum density (PSD) of $\varphi(t)$.

⋆ rubiola@polito.it
⋆⋆ giordano@lpmo.univ-fcomte.fr

Why scientists are so worried by phase noise? As this question involves many fields of science and technology, we try to answer it through some examples.

First of all, the replacement of analog circuits with digital electronics at higher and higher clock frequencies is a major technological trend. In a digital circuit the *bit*, i.e. the quantum of information, is represented as a voltage saturated to the high or low level, 1 or 0, which makes small amplitude fluctuations not so relevant. On the other hand, for proper operation digital circuits need precise timing, within a fraction of the clock period.

Secondly, we consider a synthesizer that – by definition – transforms the driving frequency ν_i into an output frequency $\nu_o = \frac{n}{d}\,\nu_i$, where n and d are integers. Restricting our attention to an ideal synthesizer consisting of zero-delay noise-free circuits, if the driving signal is affected by a time jitter δt_i, the same time jitter is present at the output. Therefore, the synthesizer transforms the input phase fluctuations $\varphi_i(t)$ into fluctuations $\varphi_o(t) = \frac{n}{d}\,\varphi_i(t)$ of the output signal. So, any attempt to increase the frequency also increases phase noise. Even worse, if the rms value of $\varphi_o(t)$ exceeds some 1 rad, the carrier vanishes due to cycle loss and extra cycle insertion at random time.

Thirdly, we consider a feedback oscillator whose nominal frequency ν_0 is set by a resonator of merit factor Q. The oscillator loop gain must be equal to 1 for the oscillation to be stable, which means unity modulus and 0° phase. In practice the oscillation frequency is determined by the 0° phase condition only, while the unity gain condition results from saturation or from amplitude control. Thus, a *phase* perturbation φ_a present along the loop path is compensated by the resonator, whose phase changes by $\varphi_r = -\varphi_a$, which produces a *frequency* change $\delta\nu = \frac{\nu_0}{2Q}\varphi_a$. The output phase error, which is the integral of $\delta\nu$, may diverge. This description of the oscillator behaviour is known as the Leeson model [1].

Finally, get a look at the long range radar. The main lobe illuminates both the target and the ground. Obviously, a pulsed radar can not discriminate between the target and the ground clutter at the same range. But fortunately the echo from a moving target is frequency shifted by $\Delta\nu/\nu_c = 2v/c$, due to the Doppler effect; v is the range rate of the target and $c = 3{\times}10^8$ m/s is the speed of light. As a consequence, a Doppler radar can divide a moving target from the clutter, but this is possible only if the source linewidth is sufficiently narrow to allow dividing the received frequency from the transmitted one; in addition, the radar oscillator must keep its frequency constant from the emission to the reception instant. Both these features rely upon the low phase noise of the oscillator and its components [2,3].

2 Background

Phase noise is a random process, and consequently its power spectrum density $S_\varphi(f)$ can only be defined as the Fourier transform of the autocorrelation

function $\mathcal{R}_\varphi(\tau)$. The one-side spectrum is preferred because this is what spectrum analyzers display. Complying to the usual terminology, we use the symbol ν for the frequency and f for the Fourier frequency, i.e. the frequency of the detected signal when the sidebands around ν are down converted to baseband.

The power-law model is most frequently used for describing phase noise. It assumes that $S_\varphi(f)$ is equal to the sum of terms, each of which varies as an integer power of frequency. Thus each term, that corresponds to a noise process, is completely specified by two parameters, namely the exponent and the value at $f = 1$ Hz. Five power-law processes, listed underneath, are common with electronics.

noise type	$S_\varphi(f)$
white phase	$b_0 f^0$
flicker phase	$b_{-1} f^{-1}$
white frequency	$b_{-2} f^{-2}$
flicker frequency	$b_{-3} f^{-3}$
random-walk frequency	$b_{-4} f^{-4}$

All these noise types are generally present at the output of oscillators, while two-port devices show white phase and flicker phase noise only. For reference, Fig. 1 reports the typical phase noise of some oscillators and devices.

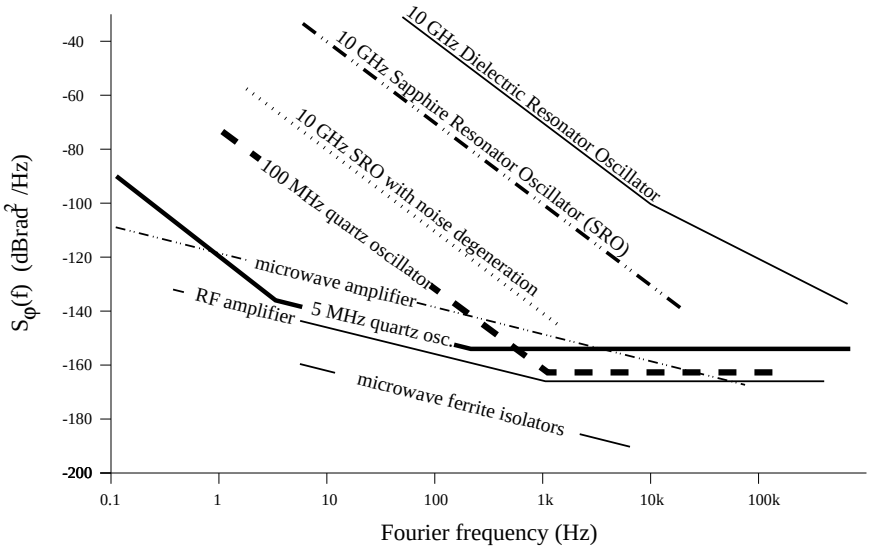

Fig. 1. Typical phase noise of some oscillators and devices

Phase noise can be measured by means of a phase-to-voltage converter in conjunction with a spectrum analyzer, which can be of the low frequency

type. On the other hand, it could be measured directly by inspecting around the carrier with a spectrum analyzer. The first method is related to the double sideband (DSB) representation of noise, while the second refers to the single sideband (SSB) representation.

2.1 Double Sideband (DSB) Representation of Noise

Let us consider a noise process of spectrum density $N(\nu)$ symmetrical around the carrier frequency ν_c, which means that $N(\nu_c+f) = N(\nu_c-f)$. That noise process is regarded as a pair of sidebands responsible for phase and amplitude noise. In order to derive $S_\varphi(f)$ we consider two symmetrical noise slots of bandwidth B at $\pm f$ apart from ν_c, as shown in Fig. 2. The rms voltage of the carrier is $\sqrt{R_0 P_c}$. The two noise sidebands must be *in quadrature* to the carrier for only the phase to be perturbed. Assuming that the noise contributes equally to amplitude and phase, the rms voltage of the *quadrature* sidebands is $\sqrt{R_0 NB/2}$. These sidebands cause a phase modulation whose peak angle is $\varphi_p = \arctan\sqrt{2NB/P_c}$, as it results from the phasor representation of Fig. 2; the corresponding phase fluctuation is $\varphi_{\rm rms} = \arctan\sqrt{NB/P_c}$. Under the assumption of low noise-to-carrier ratio, that modulation angle becomes $\varphi_{\rm rms} = \sqrt{NB/P_c}$. Hence the spectrum density is

$$S_\varphi(f) \;=\; \frac{N(\nu_c + f)}{P_c}\;. \tag{2}$$

The physical dimension of $S_\varphi(f)$ is $\mathrm{rad}^2/\mathrm{Hz}$. In addition, the technical unit $\mathrm{dBrad}^2/\mathrm{Hz}$ is frequently used.

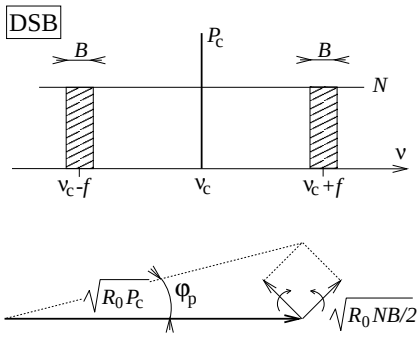

Fig. 2. Double sideband (DSB) representation of noise

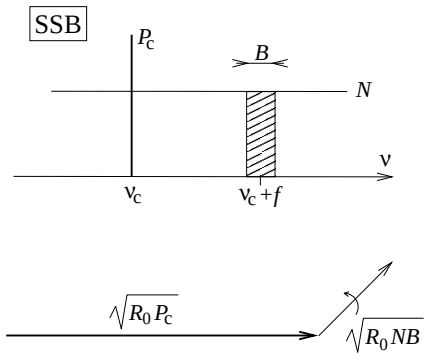

Fig. 3. Single sideband (SSB) representation of noise

In some relevant situations, the noise does *not* equally contribute to phase and amplitude. This occurs for instance with all digital circuits, in which the amplitude noise is nearly suppressed by saturation. In these cases, amplitude

and phase noise must divided and dealt with separately representing the spectrum density as $N(\nu) = N_\alpha(\nu) + N_\varphi(\nu)$. Hence, the rms voltage of the quadrature noise is $\sqrt{R_0 N_\varphi B}$ for each sideband, and consequently the phase fluctuation is $\varphi_{\rm rms} = \sqrt{2N_\varphi B/P_c}$. The phase noise spectrum density thereby obtained is

$$S_\varphi(f) \;=\; \frac{2N_\varphi(\nu_c + f)}{P_c}\;. \tag{3}$$

2.2 Single Sideband (SSB) Representation of Noise

Let us now consider one sideband of the noise process $N(\nu)$ around the carrier, as shown in Fig. 3. Taking one slot of bandwidth B at the frequency f apart from the carrier, the corresponding rms voltage is $\sqrt{R_0 N B}$. The latter causes a phase modulation $\varphi_{\rm rms} = \sqrt{NB/2P_c}$, plus an amplitude modulation. The quantity used to describe the spectrum density thereby obtained is

$$\mathcal{L}(f) \;=\; \frac{N(\nu_c + f)}{2P_c}\;. \tag{4}$$

The physical dimension of $\mathcal{L}(f)$ is Hz^{-1}; the unit of angle (rad) should be omitted. $\mathcal{L}(f)$ is usually expressed in dBc/Hz, where "c" is intended to remind that the $\mathcal{L}(f)$ results from the noise referred to the carrier power.

Assuming that noise contributes equally to phase and amplitude modulation, for small modulation angles it holds $\mathcal{L}(f) = \frac{1}{2}\, S_\varphi(f)$.

It should be noticed that the above derivation of (4) does not contain any explicit reference to phase, while phase noise comes from the equipartition of noise between the two degrees of freedom, i.e. phase and amplitude. Obviously, whenever the equipartition does not apply – as it occurrs with frequency multiplication – definition (4) yields a misleading result. In addition, nowadays $\mathcal{L}(f)$ is almost always measured by means of a phase to voltage converter, which is insensitive of amplitude. For this reason, the definition (4) is now being changed [4] into

$$\mathcal{L}(f) \;=\; \frac{1}{2}\, S_\varphi(f)\;. \tag{5}$$

Finally, $\mathcal{L}(f)$ is preferred to $S_\varphi(f)$ by most manufacturers; nevertheless, we use $S_\varphi(f)$ because we find it more clear.

3 Traditional Methods

The double balanced mixer (DBM), used as a phase-to-voltage converter as shown in Fig. 4, is the main tool for phase noise measurements. The mixer is driven by two signals in quadrature ($\gamma = 90°$) with nearly equal power

$$r(t) = \sqrt{2R_0 P_c}\cos\left[2\pi\nu_c t + \gamma\right] \tag{6a}$$

$$s(t) = \sqrt{2R_0 P_c}\;\left[1 + \alpha(t)\right]\cos\left[2\pi\nu_c t + \varphi(t)\right]\;. \tag{6b}$$

Basically, the mixer is a multiplier. Thus the signal at the output of the lowpass filter is $[r(t)s(t)] * h_{\rm lp}(t) = R_0 P_c[1 + \alpha(t)] \sin[\varphi(t)]$; the symbol '$*$' stands for the convolution operator and $h_{\rm lp}(t)$ is the low pass function that eliminates the $2\nu_c$ component of the IF signal. For proper operation, the mixer is saturated at both inputs. Hence the output signal is independent of the input power, and the amplitude noise $\alpha(t)$ vanishes. Linearizing $\sin(\varphi)$ for small φ, the output signal is

$$v(t) = \sqrt{K_\varphi}\, \varphi(t) \tag{7a}$$

$$S_v(f) = K_\varphi\, S_\varphi(f)\ , \tag{7b}$$

which also defines the power gain K_φ. For commodity we tend to use either K_φ or $k_\varphi = \sqrt{K_\varphi}$, depending on the measurement method; anyway, the numerical value in dB is the same.

Obviously, the measurement of $S_v(f)$ gives $S_\varphi(f)$. Often, the fast Fourier transform (FFT) analyzer is the most suitable instrument because of the wide dynamic range, typically of some 80–90 dB.

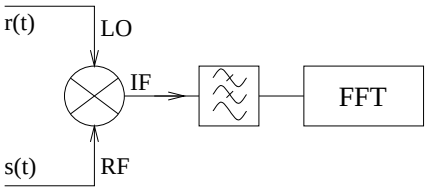

Fig. 4. Basic scheme of the traditional phase noise measurement system

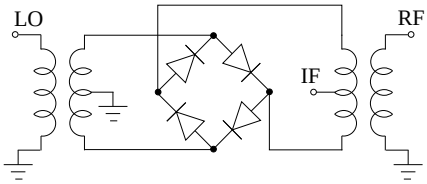

Fig. 5. Scheme of a typical radiofrequency double balanced mixer

The double balaced mixer can take various forms [5–7], depending on frequency and technology. Figure 5 shows the scheme most widely used in the HF to UHF bands (bands 7 to 9).

3.1 Instrument Sensitivity

The white noise limit comes from the input noise of the amplifier inserted between the mixer and te spectrum analyzer (not shown in Fig. 4), In fact, commercial FFT spectrum analyzers show a typical input noise of the order of 20 $\mathrm{nV}/\sqrt{\mathrm{Hz}}$, limited by the relatively high input impedance. On the other hand, the mixer output impedance is low, typically 50 Ω. Consequently, the sensitivity can be significantly improved by inserting an amplifier with lower input impedance between the mixer and the analyzer. The input noise $S_{v0}(f)$ of that amplifier can be of 1 $\mathrm{nV}/\sqrt{\mathrm{Hz}}$ (−180 dBV) or lower [8]. In this conditions, assuming that $K_\varphi = -10$ $\mathrm{dBV}^2/\mathrm{rad}^2$, a noise floor of −170 $\mathrm{dBrad}^2/\mathrm{Hz}$ can be attained. This high sensitivity refers to good or best conditions only.

It should be remarked that the best noise impedance $R_b = \sqrt{S_v(f)/S_i(f)}$ of the operational amplifiers is in the kΩ range; $S_v(f)$ and $S_i(f)$ refer to the spectral density of the voltage and current noise of the amplifier. For this reason, the operational amplifiers are misused when connected to a mixer that shows an output impedance as low as 50 Ω.

The flicker noise of the instrument comes from the mixer diodes, and it is insufficiently documented in the literature. According to our experience, the actual limit turns out to be of some -140 dBrad^2/Hz, depending on the mixer type and the driving power. The flicker of a low noise amplifier can be lower than 3 nV/$\sqrt{\text{Hz}}$ at $f = 1$ Hz, i.e. -170 dBV, which is negligible compared to the mixer noise.

Figure 6 shows the typical limit of the phase noise measurement system based on the double balanced mixer.

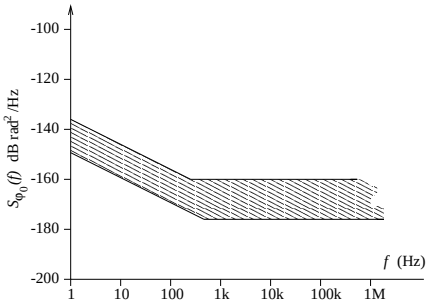

Fig. 6. Typical instrument noise of a mixer based phase noise measurement system

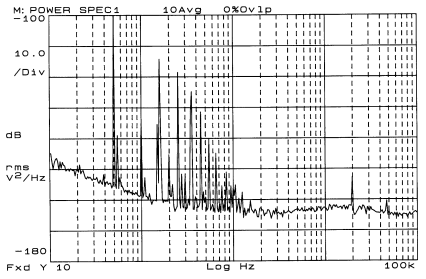

Fig. 7. Example of instrument noise $S_{\varphi 0}(f)$, measured in the absence of the device to be tested. Vertical scale is dBrad^2/Hz

3.2 Additional Instrument Limitations

Due to disturbances from the mains, the measured spectrum includes many lines at 50 Hz (or the appropriate frequency, out of the Europe) and multiples. These disturbances are picked up at the input of the operational amplifier, where the signal level is the lowest. Signal processing is only partially useful to clean up the measurement results because the spectrum analyzer shows a finite bandwidth, and consequently two contiguous harmonics of the mains may hide the useful information in between, thus limiting the sensitivity. Figure 7 provides a typical example of actual results.

The mixers designed for radiofrequency bands are based on ferrite tore transformers and Schottky diodes. They show a bandwidth of up to 3 decades in the region from 20 kHz to 2 GHz approximately. At higher frequencies, the transformer is replaced with a microstrip network, whereat the bandwidth

is limited to 1–3 octaves. The maximum operating frequency is of the order of 40 GHz, although some special devices may be usable up to 100 GHz, or even beyond.

The adoption of a saturated mixer as the phase-to-voltage converter turns into a severe limitation of the instrument power range. The conversion gain is roughly proportional to driving power. Accounting for the diode saturation level and maximum power, the useful dynamic range tends to be of some 10 dB. Mixers are hardly usable below approximately 5 dBm, while flicker noise increases as the power approaches the maximum value.

4 Useful Schemes

Figures 8 to 15 show some experimental configurations that cover most practical needs.

General Two Port Devices. A two port device (DUT, i.e. the device under test) can be measured with the scheme of Fig. 8. This scheme is a direct application of the principles shown in Section 3. Both $r(t)$ and $s(t)$ originate from a single source, but only $s(t)$ is affected by the DUT noise. The quadrature condition is ensured by the variable phase shifter γ, that must be adjusted to compensate for the phase lag of the DUT and cables. The quadrature condition can be first checked observing the dc voltage at the mixer output, that must be 0 V. For highest accuracy, the dc offset that results from the diode asymmetry must be taken into account; a true phase measurement may be necessary instead of just trimming γ for 0 V_{dc} at the IF output.

The scheme of Fig. 8 works well if the DUT shows relatively low insertion loss because the mixer must be driven with the same level at the two inputs. In addition, the DUT group delay must be relatively small. This is necessary to ensure the rejection of the phase noise of the driving oscillator. Anyway, this problem will be explained underneath dealing with the discriminator.

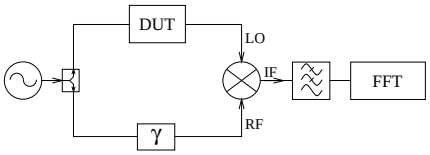

Fig. 8. Phase noise measurement of a 2 port device

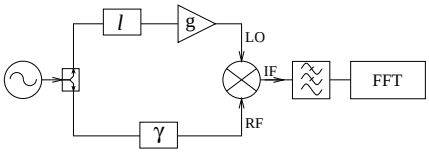

Fig. 9. Measuring an amplifier as the DUT, the amplifier must be preceeded by an attenuuator of loss ℓ equal to the gain g

Amplifiers. The phase noise of an amplifier can be measured with the scheme of Fig. 9. The amplifier gain g is compensated by an attenuator of loss $\ell \simeq g$. Obviously the attenuator and the amplifier can not be interchanged, unless the amplifier dynamics is sufficienly large to avoid saturation. Anyway, it should be noticed that the close-to-the-carrier flicker noise of the amplifier comes from the near-dc flicker of the bias current, up converted by nonliearity [9,10], and hence it strongly depends upon the output power. In addition, the presence of the attenuator increases by a factor ℓ the overall noise figure of the attenuator-amplifier compound, whereat the white noise floor of the measurement is also increased by ℓ.

High Insertion-Loss Two Port Devices. The mixer requires nearly equal driving power at the two inputs. Accordingly, if the DUT shows a significant loss ℓ, an attenuator of equal loss must be inserted in the other arm, and the oscillator power must be set to an appropriately higher value. This solution requires that the increased power is tolerated by the DUT without noise increase or damnage. Alternatively, the DUT loss can be compensated inserting an amplifier of gain $g \simeq \ell$, as shown in Fig. 10. The amplifier is also needed to measure the DUTs that must work in low power conditions. Unfortunately the power required to drive the mixer is relatively high and sufficient to make the amplifier flicker, which impairs the instrument sensitivity. For this reason some low noise devices, like the high stability quartz resonators [11], can not be measured with this scheme.

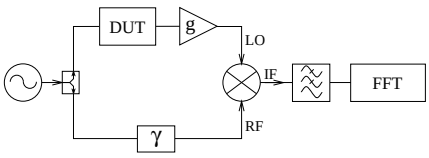

Fig. 10. In some cases an amplifier is needed to compensate for the DUT loss

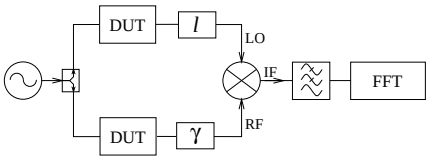

Fig. 11. Whenever possible, two equal DUTs should be measured simultaneously

Equal DUT Pair. When two equal DUTs are available, they can be inserted each in one arm of the circuit, as shown in Fig. 11. To reduce the circuit complexity, the attenuation of the variable phase shifter γ is compensated by the variable attenuator ℓ, while the phase lag of the latter is compensated by γ. If the two devices are equally noisy there results a 3 dB improvement of sensitivity.

The presence of two equal DUTs is sometimes useful to improve the rejection of the source noise by compensating for the discriminator effect of each DUT.

The scheme of Fig. 11 turns out to be useful for the measurement of frequency multipliers, dividers and synthesizers in general. In fact, if two independent oscillators were used to measure a *single* sinthesizer – one oscillator drives the synthesizer and the other one serves as the reference of the mixer – it would be necessary to use two noise-free oscillators because no rejection of the fluctuations of these oscillators would take place.

Discriminator and Delay Line. A single oscillator can be measured with the scheme of Fig. 12, in which the resonator is used as a reference frequency discriminator. The resonator responds to a frequency change $y = \frac{\nu - \nu_c}{\nu_c}$ with a phase $\varphi_m = 2Qy$, where Q is the merit factor of the resonator. Accordingly, the spectrum density $S_{\varphi m}(f)$ of the measured phase is related to the frequency fluctuation $S_{yo}(f)$ of the oscillator by

$$\begin{aligned} S_{\varphi m}(f) &= 4Q^2 S_{yo}(f) \\ &= 4Q^2 \frac{f^2}{\nu_0^2} S_{\varphi o}(f) \ . \end{aligned} \tag{8}$$

The above hold at low Fourier frequencies ($f \ll \frac{\nu_c}{2Q}$), where the resonator phase lag can be derived from a quasistatic model. For $f > \frac{\nu_c}{2Q}$, the resonator filters out the frequency fluctuations of the oscillator. These fluctuations are still present at the other input of the mixer, and therefore the instrument measures the phase noise of the oscillator.

In most cases the discriminator shows poor sensitivity, due to the insufficient Q factor of the resonator. On the other hand, the poor sensitivity turns into a wide dynamic range.

A delay line does the same work as the resonator. The equivalent merit factor is $Q_e = \pi\tau\nu_c$, where τ is the delay of the line. Unfortunately, delay lines are scarcely useful in the frequency domain of our interest because of the insufficient value of the $\tau\nu_c$ product. Nevertheless, the delay line is of great interest for optics.

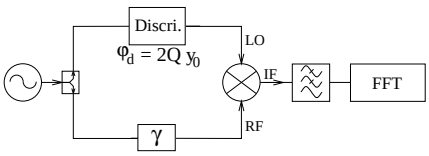

Fig. 12. A discriminator converts the frequency fluctuation of the driving oscillator into phase fluctuations that are measured by means of a mixer

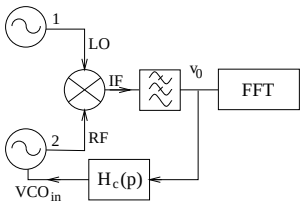

Fig. 13. Phase noise measurement of two equal oscillators

Oscillator Pair The measurement of oscillators requires a phase locked loop (PLL) as in Fig. 13 – or some other locking mechanism – otherwise it would be impossible to keep the mixer inputs in quadrature. The PLL is usually regarded as a low pass filter, in which the voltage contolled oscillator (VCO) tracks the input. The corresponding transfer function is

$$\frac{S_{\varphi 2}(f)}{S_{\varphi 1}(f)} = \frac{|k_o k_\varphi H_c(f)|^2}{4\pi^2 f^2 + |k_o k_\varphi H_c(f)|^2} \,, \tag{9}$$

where k_o is the VCO gain, given in rad/sV. In order to measure phase noise, the error signal v is used as the PLL output signal, and therefore the transfer function is

$$\frac{S_v(f)}{S_{\varphi 1}(f)} = \frac{4\pi^2 f^2 k_\varphi^2}{4\pi^2 f^2 + |k_o k_\varphi H_c(f)|^2} \,, \tag{10}$$

which is a high pass function. Obviously, the loop response must be sufficiently slow for the oscillator no. 2 *not* to track the other one.

Alternatively, the scheme of Fig. 13 can be exploited to increase the dynamic range of the system. In this case, an amplifier is inserted as the H_c block, setting the loop gain to a suitable value that pushes the high pass cutoff frequecy just below the corner of the oscillator frequency flicker.

The frequency flicker is of the f^{-3} type, while the PLL response is proportional to f^2. The combined effect yields a measured spectrum of the f^{-1} type, from which the flicker coefficient can be calculated.

The PLL scheme of Fig. 13 can be used to compare an oscillator to a reference one, considered noise free, or to compare two equal oscillators. In this case, a 3 dB factor must taken into account.

Frequency Multiplier. In some cases the frequency multiplier turns out to be a useful tool to enhance the instrument sensitivity (Fig. 14). In fact, if the frequency is multiplied by n, the phase also is multiplied by n. Hence the output power spectrum $S_{\varphi o}(f)$ is related to the input spectrum $S_{\varphi i}(f)$ by $S_{\varphi o}(f) = n^2 S_{\varphi i}(f)$. The obvious extension to the general case of the synthesizer is $\nu_o = \frac{n}{d}\,\nu_i$, which means $\varphi_o(t) = \frac{n}{d}\,\varphi_i(t)$ and conssequently $S_{\varphi_o}(f) = (\frac{n}{d})^2 S_{\varphi i}(f)$.

The multiplier contributes with its own noise, which must be lower than that of the mixer for the multiplier to be useful. In pratice this constraint turns into a serious difficulty for the white noise, but it is relatively easy to meet with the frequency flicker noise of the oscillator, whose slope is f^{-3}.

Narrow Tuning Range Oscillators. With some high quality oscillators, the tuning range is significantly narrower than the initial frequency accuracy. This occurrs when the Q factor of the resonator is extremely high, 10^6 to 10^9, and for technical reasons the resonance frequency can not be changed

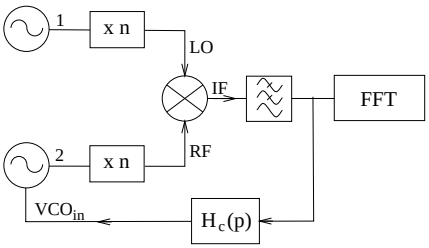

Fig. 14. Frequency multiplication enhances the instrument gain

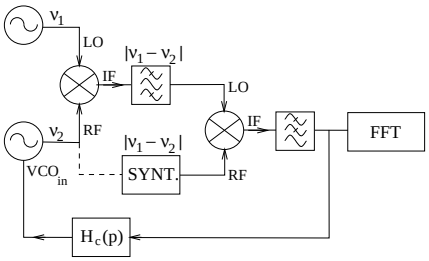

Fig. 15. Phase noise measurement of two oscillators *not* at the same frequency

with a resolution better than $\frac{\nu_c}{2Q}$. This is typical of the oscillators based on whispering gallery sapphire resonators or on cryogenic resonators. The noise of these oscillators is so low that no synthesizer would be adequate, and there is no chance to get two oscillators at the same frequency. Yet, the phase noise measurement is still possible by means of the scheme of Fig. 15. Choosing two oscillators whose frequencies are as close as possible to one another, the phase noise measurement is performed at the beat frequency $\nu_d = |\nu_1 - \nu_2|$, by comparison with an auxiliary synthesizer.

The configuration of Fig. 15 shows an additional advantage as it prevents the measurement error due to injection locking. In fact, when high Q resonators are used, the oscillators tend to lock to one another if the frequencies are sufficiently close.

5 Interferometric Noise Measurement Method

It has been shown in Section 3 that the saturated mixer used as a phase-to-voltage converter suffers from three basic problems, namely the narrow power range, the flicker noise of the mixer, and the relatively high white noise floor due to the poor phase-to-voltage conversion gain. An improved solution consists of the interferometric scheme, shown in Fig. 16. This scheme, inspired to [12], has been subsequently ameliorated and extended to the HF and VHF bands [13].

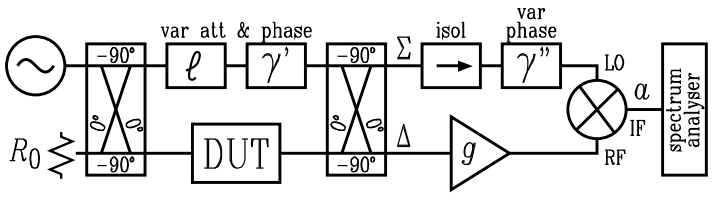

Fig. 16. Basic scheme of the radiofrequency interferometer

The left hybrid is used as a power splitter. It should be remarked that actual two way power splitters are 4 port hybrids with one port terminated to an internal resistor, otherways they could not be impedance matched; for details on these devices consult [14]. The right hybrid coupler makes the vector addition, i.e. the *interference* of its input signals. Thus, setting ℓ' and γ' so that the two paths from the oscillator to the Δ output of that hybrid are equal in amplitude and opposite in phase, all the oscillator power goes to the Σ output, while the carrier is suppressed at the Δ output. The DUT noise sidebands, which are not suppressed by the interference mechanism, are amplified by the low noise amplifier and downconverted to baseband by the mixer. After filtering out the $2\nu_c$ component, the instant voltage at the mixer output is

$$v(t) = k\,[\varphi(t)\sin\gamma'' + \alpha(t)\cos\gamma'']\ . \tag{11}$$

Thus the mixer detects PM noise, AM noise or a combination of them, depending on the detection phase γ''. Because of the particular type of conversion, the instrument gain k is written without the index φ.

Let us now introduce the following symbols

$N_\varphi(\nu)$	the power spectrum density (PSD) of the quadrature noise at the DUT output, around the carrier frequency ν_c,
$N_\alpha(\nu)$	the PSD of the in-phase noise at the DUT output, around the carrier frequency ν_c,
ℓ_h	the power loss of the hybrid, not including the 3 dB intrinsic loss. Therefore, driving one input with a power P, a power $P/2\ell_h$ is expected at each output,
ℓ_m	the power loss of the mixer, icluding the 3 dB intrinsic loss. Hence, driving the RF input with a power P, a power P/ℓ_m is expected in each output band,
R_0	the mixer output impedance,
g	the power gain of the amplifier.

A few words are to be spent about the contrast between the definition of ℓ_m, that includes the 3 dB intrinsic loss of the mixer, and the definition of ℓ_h, that does *not* include the 3 dB intrinsic loss of the hybrid. Apart from the fact that the physical origin of the intrinsic losses is not the same, the above definitions of ℓ_m and ℓ_h are consistent with the technical documentation of most commercial components.

From the scheme of Fig. 16, the noise PSD is

$$S_\Delta(\nu) = \frac{N_\varphi(\nu) + N_\alpha(\nu)}{2\,\ell_h} \tag{12}$$

at the Δ output of the hybrid, and

$$S_{\mathrm{RF}}(\nu) = g\,\frac{N_\varphi(\nu) + N_\alpha(\nu)}{2\,\ell_h} \tag{13}$$

at the RF input of the mixer.

The noise behaviour of actual DUTs is such that the sidebands are symmetrical with respect to the carrier, which means that $N_\varphi(\nu_c - f) = N_\varphi(\nu_c + f)$ and $N_\alpha(\nu_c - f) = N_\alpha(\nu_c + f)$. Hence, the DUT noise down converted to baseband is

$$S_V(f) = \frac{2R_0 g}{\ell_h \ell_m} \left[N_\varphi(\nu_c + f) \sin^2 \gamma'' + N_\alpha(\nu_c + f) \cos^2 \gamma'' \right] . \tag{14}$$

Still assuming the sideband symmetry, the PM noise is related to N_φ by

$$S_\varphi(f) = 2 \frac{N_\varphi(\nu_c + f)}{P_c} . \tag{15}$$

If γ'' is set to 90°, combining the two above equations with the instrument gain $K_\varphi = S_V(f)/S_\varphi(f)$, we obtain

$$K_\varphi = \frac{R_0 g P_c}{\ell_h \ell_m} . \tag{16}$$

The expected noise floor of the instrument can be easily derived as follows. We first remove the DUT, replacing it with a cable; obviously, ℓ' and γ' must be set to 0 dB and 0° respectively. The carrier suppression is still effective, and the whole circuit is still impedance matched. As a consequence, the thermal noise present at the input of the amplifier comes from the termination R_0 of left side hybrid.

Accounting for the amplifier noise figure F, the equivalent noise density at input of the amplifier is $S_{\Delta 0} = F_a k_B T_0$, where $k_B = 1.38 \times 10^{-23}$ W/Hz is the Boltzmann constant, and $T_0 = 290$ K is the absolute reference temperature. It is assumed that the temperature of the interferometer is close to T_0. Thus, the voltage noise at the mixer output is

$$S_{V0}(f) = 2 \frac{R_0 g}{\ell_m} F k_B T_0 . \tag{17}$$

Assuming that the carrier is perfectly suppressed at the input of the amplifier, the amplifier noise $F k_B T_0$ can *not* be related with the phase of the carrier. Accordingly, $F k_B T_0$ gives equal contributions to phase and amplitude noise. Hence, combining (16) with (17) we obtain the phase noise floor

$$S_{\varphi 0}(f) = 2\ell_h \frac{F k_B T_0}{P_c} . \tag{18}$$

Quite a similar development yields the AM noise floor

$$S_{\alpha 0}(f) = 2\ell_h \frac{F k_B T_0}{P_c} . \tag{19}$$

The practical consequences of the above theory can be better understood through the following example.

Design Example 1. We assume that $\ell_h = 0.5$ dB and $\ell_m = 6$ dB, which are typical values for hybrids and mixers. We choose a $g = 37$ dB amplifier and we set the driving power for $P_c = 15$ dBm at the DUT output. From equation (16) we get $K_\varphi = 32$ dBV^2/rad^2. Assuming that the noise figure of the amplifier is $F = 2$ dB, equation (18) yields $S_{\varphi 0} = -185$ dB rad^2/Hz. These results compare favorably to the performance of a traditional system based on a saturated mixer that operates in similar conditions. The interferometer shows a gain 42 dB higher and a noise floor 15 dB lower.

5.1 Design Strategies

Whereas the potential benefit of high carrier suppression is clear, a suppression specification can hardly be drawn. This occurs because the interferometer takes benefit of some features of the electronic components that are not adequately documented. Therefore, we can only give some hints derived from experience.

1. The amplifier gain g should be in the 20–40 dB range. Higher values make a sufficient carrier suppression difficult to achieve, while lower values cause the mixer noise to be taken in, impairing the sensitivity.
2. The residual carrier power at the amplifier output must be much lower than the maximum amplifier power P_m; the latter is usually specified as the "1 dB compression level". A margin $P_m/(gP_r)$ of 35–40 dB or more is needed, depending on the amplifier; P_r is the residual carrier power at the amplifier input.
3. The close-to-the-carrier flicker of the amplifier results from the combined effect of near-dc flicker and nonlinearity. Although we have no information on the former, we can infer the latter from the 3rd harmonic intercept power, which is always specified for commercially available amplifiers. Obviously, the devices showing the highest intermodulation intercept power tend to be the best ones.
4. For a given configuration, flicker noise of the amplifier is entierly determined by the power available at the output of the amplifier, that is mostly due to the residual carrier. As a consequence, the suppression ratio P_c/P_r should be regarded just as a way to specify P_r, rather than a parameter relevant by itself.
5. The presence of a low noise amplifier precedig the mixer relaxes the noise specifications for the latter.

Let us consider two examples.

Design Example 2. The amplifier shows $g = 40$ dB, $P_m = 15$ dBm and needs a power margin $P_m/(gP_r) = 35$ dB for full linearity. In this condition, P_r must be less than –60 dBm. Consequently, if the DUT output power is $P_o = 15$ dBm than a carrier suppression of 75 dB must be ensured.

Design Example 3. With the same instrument of the example 2, we now measure the phase noise of two piezoelectric quartz resonators, each dissipating $P_d = 10$ μW. For this purpose we insert two equal DUTs, one in each arm of the interferometer. Each DUT is a text fixture consisting of a resistive matching network that incorporates one quartz. The DUT output power is of the same order of P_d, depending on the test fixture network. Hence, assuming $P_c = -20$ dBm, a carrier suppression of 40 dB would be sufficient.

For referece, a carrier suppression of 80 dB results from an error $\delta\gamma' = 100$ μrad of the phase shifter, *or* from an error $\delta\ell = 8.7{\times}10^{-4}$ dB of the variable attenuator. Accounting for both, the accuracy specification is even more stringent.

Microwave Design. Phase matching is the greatest technical difficulty at microwave frequencies. In fact, because the wavelength inside cables is about 22 mm at 10 GHz, a phase matching within 100 μrad – that is necessary for a carrier suppression of for 80 dB – is equivalent to an electrical length matching within 0.4 μm. Obviously, phase matching must be stable at that level for the duration of the experiment, say half an hour. Some commercially available phase shifters are adequate to do so, after a really patient adjustment.

A low instrument noise requires particular care with mechanical vibrations. In fact, at 10 GHz a noise floor of -180 dBrad^2/Hz corresponds to an electrical length fluctuation of $4{\times}10^{-12}$ m/$\sqrt{\text{Hz}}$. According to our experience, a sufficient stability can be obtained by fixing all the parts onto an antivibrating table – of the same type of those commonly used for optics – and securing to the table all the cables connecting the system to the external world.

Microwave hybrids and mixers show poor isolation, typically of the order of 20 dB. The obvious consequence is an unwanted feedback of the amplified signal through the mixer and the hybrid. In order to prevent oscillation or measurement alteration, isolation must be increased by inserting some ferrite isolators; the best configuration must be determined experimentally.

Microwave amplifiers show a wide bandwidth, in some cases more than 10 GHz. Noise integrated over such a wide band can push the amplifier out of linearity. If, for example, the amplifier shows a noise figure $F = 2$ dB, a gain $g = 40$ dB, and a bandwidth $B = 10$ GHz, the total integrated noise is $P_n = Fk_BT_0gB = -32$ dBm. Unfortunately, saturation is due to the peak power, which is some 20 dB higher than P_n. A bandpass filter can be needed.

VHF and HF Design For technical reasons, the 5–10 MHz quartz oscillator exhibits the lowest frequency flicker, compared to similar devices at other frequencies. Besides, the quartz oscillator exhibits the lowest white noise floor

when crystal resonates around 100 MHz. Therefore, a great effort is wortly to be spent to characterize the electronic devices designed for these frequencies.

Phase matching, phase stability, and a sufficient damping of mechanical vibrations are much easier to achieve than in the microwave bands because the wavelength is 10^2–10^3 times longer. The adoption of semirigid cables, SMA type connectors and antivibrating table ensures sufficient stability. Working at $\nu_c = 10$ MHz, a 120 mm thick sand layer proved to be sufficient to damp the vibrations of the floor if some care were spent to do the measurements at certain hours, when only a few people were present in the laboratory.

In spite of the apparent simplicity, for a series of reasons the design for the HF and VHF bands turns out to be more difficult than that for the X band.

The most difficult problem arises from the variable phase shifters. Some microwave devices, consisting of a transmission line whose length can be varied by means of a micrometer, proved to be a bad choice. Apart from the small delay range (0.1–1 ns), that can be extended with a set of calibrated cables, these phase shifters turned out to be scarcely useful because of their high flicker noise; the same devices work successfully in the microwave range. We guess that this anomalous behaviour could be due to the parasitic capacitance in parallel with non-perfect contacts, which behaves as short circuit at 10 GHz and takes in acoustic noise when used at 100 MHz. Presently, a type of phase shifter specific for this application, based on a LC network with a variable capacitance, is the best known solution.

Variable attenuators suitable to the VHF band are generally based on potentiometers and for this reason they tend to flicker more than the microwave ones, based on movable absorbing surfaces. We are still searching for a more satisfactory solution, consisting either of better potentiometers or a different physical principle.

It should be remarked that the flicker performance of variable attenuators and phase shifters is usually not documented in the device specifications, and consequently the possibility to find low noise devices relies upon experience and a pinch of good luck.

Eliminating the harmonics at frequencies multiple of ν_c is a critical point because the carrier suppression mechanism has no effect on them. As almost all the components show a bandwidth of 2–3 decades, these unwanted signals would be present in the entire circuit, pushing the amplifier out of linearity and making it flicker. The only known solution consists of inserting low Q bandpass filters in certain points of the circuit.

Ferrite isolators are not available for the HF and VHF bands and must be replaced with active isolators. Although noise is not critical at the Σ output of the hybrid, where the isolators are to be placed, it is really important to drive both the active isolator and the mixer at the appropriate power level.

The presence of electromagnetic pollution can be a relevant problem at some frequencies. In fact, in highly populated areas of Europe and the U.S.A.

– well covered by FM broadcastings – the electromagnetic field is often of the order of +100 dBμV/m in the 88–108 MHz band. Besides, the Ethernet – that is probably the most popular standard for local area network – operates either at 10 Mb/s or 100 Mb/s and for this reason it turns into a source of pollution particularly difficult to eliminate from some experiments. Solutions are strongly dependent on the local situation, as well as the design.

Finally, the design for the measurement of quartz crystal resonators, that shows high Q factor and operate at low power, is subject to specific design rules [15,16].

5.2 Further Remarks

The scheme of Fig. 16 can be improved by deriving the mixer LO signal from the oscillator instead of taking it at the Σ output of the hybrid. This makes the mixer pump level independent of the DUT power.

Working in the microwave bands, the 90° hybrids turn out to be the best choice. They are cheaper, smaller, and show better isolation and insertion loss than the 180° ones. The bandwidth of a 90° hybrid can be of 1–3 octaves, depending on the design and on the device size. The HF and VHF hybrids are based on lumped parameter networks. Hence, in these bands the 180° hybrids are superior to the 90° ones with respect to loss, isolation, size and cost. In addition, the 180° hybrids show a typical bandwidth of 2 decades, while the bandwidth of the 90° devices is of the order of half an octave.

In our experience the low frequency magnetic fields originated from the mains turn into a serious design problem because copper shields are not effective at these frequencies. The traditional systems, of the type described in Sections 3 and 4, are prone to that kind of disturbances because the signal, i.e. the DUT noise, is first down converted and then amplified; therefore the smallest signal, that is present at the mixer output, is a baseband one. Magnetic shielding can be used, but this solution makes the whole instrument more complicated. By contrast, the interferometer can be more effectively shielded. This occurs because the smallest signal, that consists of noise sidebands around the carrier, is amplified *before* being down converted. Moreover, low frequency magnetic fields have no effect on the high frequency noise sidebands. Figure 17, taken from [13], shows an example of instrument noise of an interferometer operating at $\nu_c = 9.1$ GHz with a carrier power $P_c = 15$ dBm. The residual of the mains can hardly be distinguished from the instrument noise.

Finally, it should be remarked that the interferometer provides the instant value of $\varphi(t)$ in real time, which makes it suitable to the dynamical removal of noise by means of a voltage controlled phase shifter in closed loop [17].

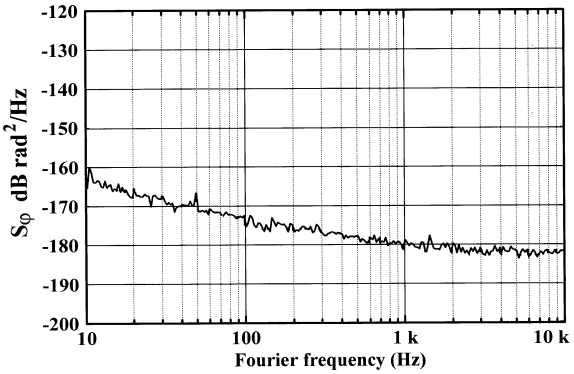

Fig. 17. Noise floor of a microwave interferometer prototype operating at $\nu_c = 9.1$ GHz. The DUT output power is 15 dBm

6 Correlation Techniques

The noise limitation of the traditional saturated mixer can be partially overcome by exploiting a correlation technique, in which two equal mixers measure the same noise process at the same time, as shown in Fig. 18. This type of measurement extracts the shared-path noise and rejects the single-arm noise processes, provided that they are independent. Obvously, the scheme of Fig. 18 can be easyly modified to measure oscillators, amplifiers, synthesizers etc., taking example from the single mixer schemes described in Section 4 (Figures 8 to 15).

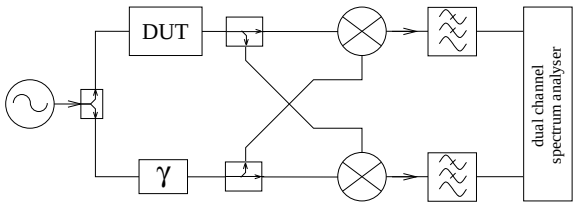

Fig. 18. Basic dual mixer correlation scheme

Searching back through the bibliography, the correlation scheme was probably used for the first time in the early '60s to measure the phase noise of hydrogen masers [18]. The dual channel correlation spectrum analyzers were not available at that time, and the correlation was evaluated through a calorimetric method. Since there, similar schemes were reproposed with updated technologies; see, for example, [19,20].

The (cross) correlation function $\mathcal{R}_{ab}(\tau)$ of two random voltages $a(t)$ and $b(t)$ is defined as

$$\mathcal{R}_{ab}(\tau) = \lim_{\theta\to\infty} \frac{1}{\theta} \int_{\theta} a(t)\, b^*(t-\tau)\, \mathrm{d}t \ , \tag{20}$$

where the symbol "$*$" stands for complex conjugate and can be omitted because we deal with real signals. The Fourier transform of $\mathcal{R}_{ab}(\tau)$ is the cross spectrum density

$$S_{ab}(f) = \int_{\infty} \mathcal{R}_{ab}(\tau) \exp(-2\pi f\tau)\, \mathrm{d}\tau \ . \tag{21}$$

Dynamic signal analyzers usually evaluate the cross spectrum density through the property

$$S_{ab}(f) = \mathcal{F}\{a(t)\}\ \mathcal{F}\{b(t)\} \ , \tag{22}$$

that holds for real signals; $\mathcal{F}\{.\}$ is the Fourier transform operator. The mathematics used in this section is clearly preseted in [21].

The signals $a(t)$ and $b(t)$ are proportional to the instant phase of the DUT, plus a random component due to the single-arm noise. Averaging on m measures, a rejection of the single-arm noise spectrum density by a factor $2\sqrt{m}$ is expected. The ultimate noise limit of the dual mixer method is not be discussed here. The noise theory of the double interferometer, that is a more sensitive instrument based on the correlation, is be given instead.

6.1 Double Interferometer

An improved version of the correlation scheme, first proposed in [22], makes use of two equal interferometers that simultaneously measure the phase noise of a shared device, as shown in Fig. 19. The spectrum analyzer rejects the noise of the individual interferometers, under the assumption that the corresponding processes are independent.

The two low noise amplifiers of Fig. 19 are impedance matched, which implies that thermal noise is present at their input. In the absence of the DUT – the latter is replaced with a short cable – all the thermal noise comes from the terminations R_1, R_2 and R_3 of the hybrids used as power splitters. Because the noise coming from R_1 R_2 and R_3 is shared by the two amplifiers, at first sight one could believe that the thermal noise limits the instrument sensitivity. The full explanation, derived from [23] and explained underneath, is much more complex.

6.2 Noise Theory of the Double Interferometer

In order to derive the noise theory of the double interferometer we analyze the case in which an attenuator of loss ℓ is inserted as the DUT. Then we define six

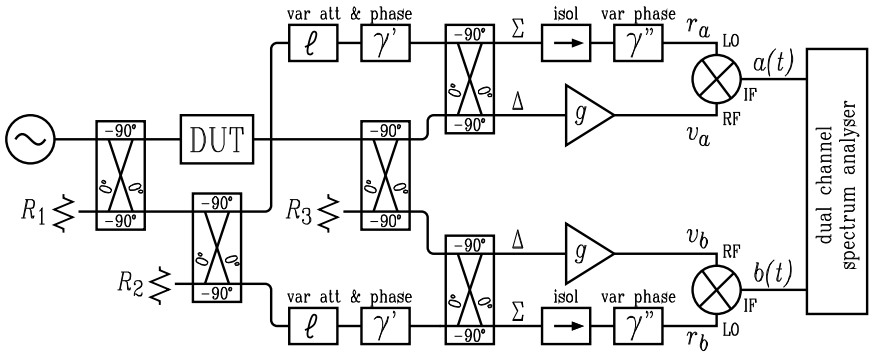

Fig. 19. Scheme of the double interferometer

thermal noise processes indicated with $n_1(t)$, $n_2(t)$, ..., $n_6(t)$, each of which coming from a resistor of value R_0, i.e. the characteristic impedance of the whole circuit. n_1, n_2 and n_3 are the available noise voltages across the resistors R_1, R_2 and R_3, respectively. n_4 and n_5 are the equivalent thermal noise of the resistive network of the variable attenuators, while n_6 is the equivalent thermal noise due to the resistive loss of the DUT. The power spectrum density $N_i(f)$ of each of these processes is equal to $R_0 k_B T_0$. The temperature of the whole instrument is assumed to be close to T_0, uniform and constant. As the DUT is an attenuator, it attenuates by ℓ any signal present at its input, including the thermal noise. As a consequence, only a fraction $\sqrt{(\ell-1)/\ell}\, n_6$. of the DUT noise n_6 is present at the output. This occurs because the total output noise at the attenuator output must be $R_0 k_B T_0$ when the attenuator input is terminated to a resistor. Similarly, the noise contributions of the two variable attenuators are $\sqrt{(\ell-1)/\ell}\, n_4$ and $\sqrt{(\ell-1)/\ell}\, n_5$. In addition, we assume that the DUT adds *extra noise* $\check{n}_6$ that can be of any type, including flicker. We use the word "extra" deliberately avoiding "excess" because the latter tend to be used as a synonym of flicker. Under the above hypotheses, the DUT output noise is

$$n_{\mathrm{dut}}(t) = \sqrt{\frac{\ell-1}{\ell}}\, n_6(t) + \check{n}_6(t)\ . \tag{23}$$

In the vicinity of the carrier frequency, a noise process can be divided in in-phase and quadrature components as

$$n(t) = n_x(t)\cos(\omega t) - n_y(t)\sin(\omega t)\ . \tag{24}$$

As we deal with thermal noise, the PSDs of the *baseband* noise processes $n_x(t)$ and $n_y(t)$ are $N_x(f) = R_0 k_B T_0$ and $N_y(f) = R_0 k_B T_0$, so that the PSD of the radiofrequency process $n(t)$ is $N(f) = R_0 k_B T_0$. Taking the oscillator signal $V\cos(\omega t)$ as the phase reference, the DUT output signal is $\sqrt{2R_0 P_c}\sin(\omega t)$. This means that the x noise component is responsible for phase noise; accordingly, $S_\varphi(f) = N_x(f)/R_0 P_c$.

For the sake of simplicity, we neglect the loss ℓ_h of the hybrids and power splitters, and the amplifier noise. The former can be introduced subsequently, and the latter vanishes in the correlation function because the two amplifiers are independent.

The reference signals at the mixer LO ports are of the form

$$r_a(t) = -V_p \cos(\omega t) \tag{25a}$$

$$r_b(t) = V_p \sin(\omega t)\ . \tag{25b}$$

Consequently, arm a detects the $\cos(\omega t)$ signal, while arm b detects the $\sin(\omega t)$ component. Due to the circuit phase relationships, the signals at the mixer RF inputs are

$$v_a(t) = \sqrt{g}\ \left[-\frac{1}{\sqrt{2\ell}}\, n_{1x} + \frac{1}{2\sqrt{\ell}}\, n_{2x} + \frac{1}{2}\, n_{3y} + \sqrt{\frac{\ell-1}{2\ell}}\, n_{4x} + \right.$$
$$\left. - \frac{1}{2}\sqrt{\frac{\ell-1}{\ell}}\, n_{6x} - \frac{1}{2}\, \check{n}_{6x} \right] \cos(\omega t) + \sqrt{g} \left[\begin{array}{c} \text{non} \\ \text{detected} \\ \text{terms} \end{array} \right] \sin(\omega t) \tag{26a}$$

$$v_b(t) = \sqrt{g}\ \left[\frac{1}{\sqrt{2\ell}}\, n_{1x} + \frac{1}{2\sqrt{\ell}}\, n_{2x} + \frac{1}{2}\, n_{3y} - \sqrt{\frac{\ell-1}{2\ell}}\, n_{5x} + \right.$$
$$\left. + \frac{1}{2}\sqrt{\frac{\ell-1}{\ell}}\, n_{6x} + \frac{1}{2}\, \check{n}_{6x} \right] \sin(\omega t) + \sqrt{g} \left[\begin{array}{c} \text{non} \\ \text{detected} \\ \text{terms} \end{array} \right] \cos(\omega t)\ . \tag{26b}$$

After filtering out the 2ω components, the detected signals present at the IF output of the mixers are

$$a(t) = \sqrt{\frac{2g}{\ell_m}}\ \left[\frac{1}{\sqrt{2\ell}}\, n_{1x} - \frac{1}{2\sqrt{\ell}}\, n_{2x} - \frac{1}{2}\, n_{3y} + \right.$$
$$\left. - \sqrt{\frac{\ell-1}{2\ell}}\, n_{4x} + \frac{1}{2}\sqrt{\frac{\ell-1}{\ell}}\, n_{6x} + \frac{1}{2}\, \check{n}_{6x} \right] \tag{27a}$$

$$b(t) = \sqrt{\frac{2g}{\ell_m}}\ \left[\frac{1}{\sqrt{2\ell}}\, n_{1x} + \frac{1}{2\sqrt{\ell}}\, n_{2x} + \frac{1}{2}\, n_{3y} + \right.$$
$$\left. - \sqrt{\frac{\ell-1}{2\ell}}\, n_{5y} + \frac{1}{2}\sqrt{\frac{\ell-1}{\ell}}\, n_{6x} + \frac{1}{2}\, \check{n}_{6x} \right]\ . \tag{27b}$$

Substituting the expression (27a) and (27a) in the definition (20), all the cross terms vanish. Hence the cross spectrum density is

$$S_{ab}(f) = \frac{g}{\ell_m}\ \left[\frac{1}{\ell}\, N_{1x} - \frac{1}{2\ell}\, N_{2x} - \frac{1}{2}\, N_{3y} + \frac{\ell-1}{2\ell}\, N_{6x} + \frac{1}{2}\, \check{N}_{6x} \right]\ . \tag{28}$$

Under the hypothesis of temperature uniformity, it holds $N_i = R_0 k_B T_0$ for all $i = 1 \ldots 6$. Consequently most of the terms of (28) cancel with one another and there results

$$S_{ab}(f) = \frac{g}{2\ell_m} \check{N}_{6x}(f) \; . \tag{29}$$

The above equation states that the instrument compensates for the thermal noise, and therefore $\check{N}_{6x}(f)$ only contributes to the measured phase noise.

Finally, the gain of the double interferometer is

$$K_\varphi = \frac{gR_0P_c}{2\ell_m} \; , \tag{30}$$

which is half that of the single interferometer. This is is reasonable because in this case only half of the DUT noise is processed by each interferometer. For the same reason, the single arm noise floor is 3 dB higher than that of the single interferometer.

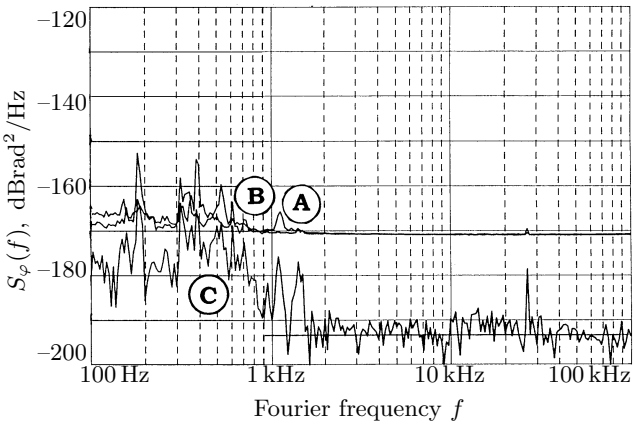

Fig. 20. Noise floor of the 100 MHz double interferometer prototype. A and B: single-arm. C: correlation

6.3 Noise Properties of the Double Interferometer

The double interferometer shows some relevant noise properties that, although quite innatural at first sight, are well predicted by the general theory.

Noise Floor. The first consequence of the thermal noise compensation mechanism is that the noise floor of the double interferometer can be lower than the thermally originated phase noise $S_{\varphi\,\mathrm{th}} = k_B T_0 / P_c$.

Figure 20 shows an example of noise floor averaged on $m = 32767$ measures. This floor refers to a prototype operating at the carrier frequency $\nu_c = 100$ MHz, and fully described in [24]. In this prototype, the amplifiers show gain $g = 40$ dB and noise figure $F = 2$ dB. The signal power at the mixer LO inputs is 8 dBm, and the DUT power is $P_c = 8$ dBm. The hybrids show losses $\ell_h = 0.8$ dB, while the mixer loss is $\ell_m = 6$ dB. Obviously, the DUT is replaced with a cable.

The single-arm noise floor (curves A and B of Fig. 20) is -172 dBrad^2/Hz, which is close to the expected value $S_{\varphi\,a}(f) = S_{\varphi\,b}(f) = 4Fk_BT_0\ell_h^2/P_c \simeq -172.3$ dBrad^2/Hz. The thermal noise calculated for the same conditions is $S_{\varphi\,\mathrm{th}} = k_BT_0/P_c \simeq -182$ dBrad^2/Hz. Yet, the measured floor (curve C) is $S_{\varphi\,0} \simeq -194$ dBrad^2/Hz, which is 12 dB lower than $S_{\varphi\,\mathrm{th}}$.

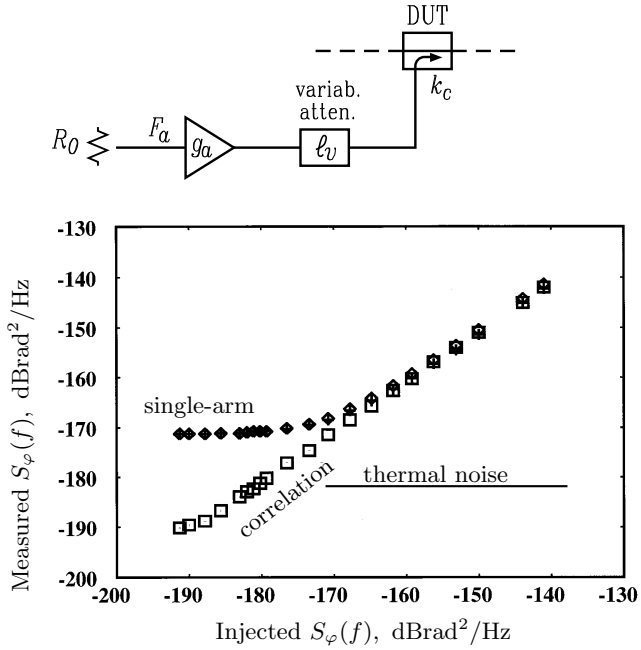

Fig. 21. Measurement of a reference noise $\check{N}_6$ injected along the DUT path

Noise Measurement Below the Thermal Floor. The possibility of measuring *extra* noise below the thermal floor can be experimented by injecting noise in the DUT path through a directional coupler, as shown in Fig. 21 (top). Neglecting the thermal noise N_6 because it is expected to be rubbed out, this circuit injects calibrated noise $\check{N}_6(f) = g_aR_0F_ak_BT_0/(\ell_vk_c)$. $\check{N}_6$ can

be set to the desired value adjusting ℓ_v. The equivalent phase noise thereby injected is $S_{\varphi i}(f) = g_a R_0 F_a k_B T_0/(\ell_v k_c P_c)$. Fig. 21 (bottom) shows the measured S_φ as a function of the injected $S_{\varphi i}$. Going to the left of that figure, ℓ_v increases and the injected noise becomes negligible compared to the equivalent noise at the amplifier inputs. Therefore, the single-arm S_φ approaches the value of -172 dBrad^2/Hz previously measured in the absence of the DUT. By contrast, the correlated noise fits the straight line $S_\varphi = S_{\varphi i}$ even below $S_{\varphi\,\mathrm{th}} = k_B T_0/P_c$.

Noise of an Attenuator. The same noise mechanism responsible for the compensation of the shared resistor noise (R_1, R_2 and R_3) is also effective on the noise of an attenuator inserted along the DUT path. Figure 22 shows two extreme situations, in which the attenuator noise is generated separately in each arm of the double interferometer (left), or in the shared path (right). Experiments performed with 16 dB attenuators show that the instrument noise floor is the same for both the configurations, that it is lower than the thermal noise, and that it is limited by the averaging size m only [23].

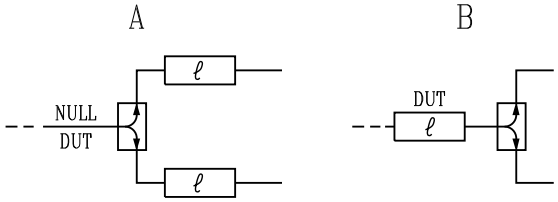

Fig. 22. Measurement schemes with independent attenuators in each arm, and with a shared attenuator. The attenuation $\ell = 16$ dB was usen in the experiments

References

1. D. B. Leeson, "A simple model of feed back oscillator noise spectrum", *IEEE Proceedings* vol. 54 no. 2 pp. 329–330, February 1966.
2. D. B. Leeson, G. F. Johnson, "Short-term stability for a Doppler radar: requirements, measurements and techniques", Proc. *IEEE-NASA Symposium on Short Term Frequency Stability* pp. 3–9, Greenbelt (MD, USA), 23–24 November 1964.
3. S. J. Goldman, *Phase noise analysis in radar systems*, John Wiley 1989, ISBN 0-471-61894-2.
4. E. S. Ferre-Pickal, J. R. Vig, J. C. Camparo, L. S. Cutler, L. Maleki, W. J. Riley, S. R. Stein, C. Thomas, F. L. Walls and J. D. White, "Draft revision of IEEE STD 1139-1988 standard definitions of physical quantities for fundamental frequency and time metrology - random instabilities", Proc. *51st Frequency Control Symposium* pp. 338–357, Orlando (FL, USA), 28–30 May 1997.

5. S. A. Maas, *Microwave mixers*, Artech House 1993, ISBN 0-89006-605-1.
6. S. A. Maas, *Nonlinear Microwave Circuits*, Artech House 1998, ISBN 0-7803-3403-5.
7. E. L. Kollberg (editor), *Microwave and millimeter-wave Mixers*, IEEE Press 1984, ISBN 0-87942-179-7
8. S. Franco, *Design with operational amplifiers and analog integrated circuits (2nd ed)*, McGraw Hill 1998, ISBN 0-07-115722-0.
9. V. N. Kuleshov, T. I. Boldyreva, "$1/f$ AM and PM noise in bipolar transistor amplifiers: sources, ways of influence, techniques of reduction", Proc. *51st Frequency Control Symposium* pp. 446–455, Orlando (FL, USA), 28–30 May 1997.
10. F. L. Walls, E. S. Ferre-Pikal, S. R. Jefferts, "Origin of $1/f$ PM and AM noise in bipolar junction transistor amplifiers", *IEEE Transactions on Ultrasonics Ferroelectrics and Frequency Control* vol. 44 no. 2 pp. 326–334, March 1997.
11. J. J. Gagnepain, "Fundamental noise studies of quartz crystal resonators", Proc. *30th Frequency Control Symposium* pp. 84–91, Atlantic City (USA), 2–4 Jun 1976.
12. K. H. Sann, "The measurement of near-carrier noise in microwave amplifiers", *IEEE Transactions on Microwave Theory and Techniques* vol. 16 no. 9 pp. 761–766, September 1968.
13. E. Rubiola, V. Giordano, J. Groslambert, "Very high frequency and microwave interferometric PM and AM noise measurements", *Review of Scientific Instruments* vol. 70 no. 1 pp. 220–225, January 1999. ISSN 0034-6748.
14. R. Mongia, I. J. Bahl, P. Bhartia, *RF and microwave coupled-line circuits*, Artech House 1999, ISBN 0-89006-830-5.
15. J. Groslambert, V. Giordano, M. Brunet, E. Rubiola, "Flicker noise measurement of HF quartz resonators", Proc. *13th European Frequency and Time Forum / 1999 Frequency Control Symposium*, Besançon (France), 12–16 April 1999. To be printed.
16. E. Rubiola, J. Groslambert, M. Brunet, V. Giordano, "Flicker noise measurement of HF quartz resonators", to be published in the *IEEE Transactions on Ultrasonics Ferroelectrics and Frequency Control*, 2000.
17. E. N. Ivanov, M. E. Tobar, R. A. Woode, "Microwave interferometry: applications to precision measurements and noise reduction techniques", *IEEE Transactions on Ultrasonics Ferroelectrics and Frequency Control* vol. 45 no. 6 pp. 1526–1536, November 1998.
18. R. F. C. Vessot, R. F. Mueller, J. Vanier, "A cross-correlation technique for measuring the short-term properties of stable oscillators", Proc. *IEEE-NASA Symposium on Short Term Frequency Stability* pp. 111–118, Greenbelt (MD, USA), 23–24 November 1964.
19. F. L. Walls, S. R. Stain, J. E. Gray, D. J. Glaze, "Design considerations in state-of-the-art signal processing and phase noise measurement systems", Proc. *30th Frequency Control Symposium* pp. 269–274, Atlantic City (NJ, USA) 2–4 Jun 1976.
20. D. Fest, J. Groslambert, J. J. Gagnepain, "Individual characterization of an oscillator by means of cross-correlation or cross covariance method", *IEEE Transactions on Instrumentation and Measurement* vol. 32 no. 3 pp. 447–450, September 1983.
21. R. N. McDonough, A. D. Whalen, *Detection of signals in noise*, Academic Press 1995, ISBN 0-12-744852-7.

22. E. Rubiola, V. Giordano, and J. Groslambert, "Double correlating interferometer scheme to measure PM and AM noise", *Electronics Letters* vol. 34 no. 1, January 8th, 1998.
23. E. Rubiola, V. Giordano, "Correlation-based noise measurements below the thermal noise floor", Proc. *13th European Frequency and Time Forum / 1999 Frequency Control Symposium*, Besançon (France), 12–16 April 1999. To be printed.
24. E. Rubiola, V. Giordano, J. Groslambert, "Improved interferometric method to measure near-carrier AM and PM noise", *IEEE Transactions on Instrumentation and Measurement* vol. 48 no. 2 pp. 642–646, April 1999.